J. Fluid Mech. (1981), *vol.* 111, *pp.* 411–420
Printed in Great Britain

Steady shallow flow over a spillway

By N. S. SIVAKUMARAN, R. J. HOSKING† AND T. TINGSANCHALI

Asian Institute of Technology, Bangkok, Thailand

(Received 14 November 1980)

A simple derivation of recent shallow-flow equations with bed curvature is presented. These equations are applied to steady flow over a high overflow spillway crest, to obtain the head–discharge relationship and the crest-pressure distribution in good agreement with experiment. It is inferred that the equations are valid for quite large negative curvature. On the other hand, their application to steady flow over a spillway toe indicates their validity for positive curvature is more limited.

1. Introduction

The well-known nonlinear shallow-flow equations of de Saint-Venant (1871) for open channels have been generalized by Dressler (1978) to account for bed curvature, i.e. when the channel bottom is not flat. With bed curvature one has to consider a vertical velocity component and the pressure is no longer simply hydrostatic. Dressler (1978) adopted curvilinear co-ordinates and carried out a detailed asymptotic analysis, retaining terms to first order in the 'shallowness parameter' to derive his equations. In §2 we note the essential assumptions involved to deduce these equations from the usual equations of flow in these co-ordinates. We deduce a more compact form of the parallel component of the equation of motion. In §§3 and 4 the equations are applied to steady flow over a high overflow spillway crest and a spillway toe, respectively.

2. Shallow-flow equations with bed curvature

Orthogonal curvilinear co-ordinates (s, n) are used to define the two-dimensional flow domain, where s is measured downstream along the bed and n is normal upwards from it, as shown in figure 1. Scale factors for these co-ordinates are $1-\kappa n = J(s,n)$ and 1 respectively, where $\kappa(s)$ and $J(s,n)$ denote curvature and Jacobian. We consider incompressible irrotational inviscid flow under constant gravity g, so that the system of equations to be solved is:

$$\frac{\partial u}{\partial s}+\frac{\partial}{\partial n}(Jw)=0, \quad \frac{\partial}{\partial n}(Ju)=\frac{\partial w}{\partial s}, \tag{2.1), (2.2}$$

$$\frac{1}{g}\frac{\partial u}{\partial t}+\frac{1}{J}\frac{\partial E}{\partial s}=0, \quad \frac{1}{g}\frac{\partial w}{\partial t}+\frac{\partial E}{\partial n}=0, \tag{2.3), (2.4}$$

† Permanent address: University of Waikato, Hamilton, New Zealand.

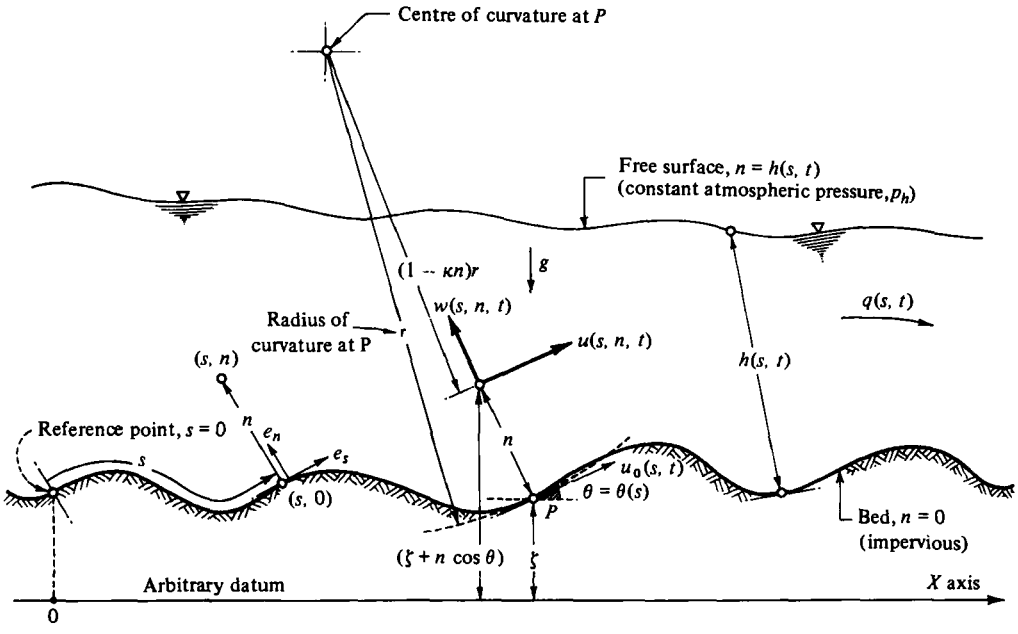

FIGURE 1. Definition sketch.

$$\frac{\partial h}{\partial t}+\frac{u}{J}\frac{\partial h}{\partial s}=w \quad \text{at} \quad n=h(s,t), \tag{2.5}$$

$$w(s,0,t)=0, \quad p(s,h,t)=p_h, \tag{2.6), (2.7}$$

where the energy profile

$$E=E(s,n,t)=\zeta+n\cos\theta+\frac{p}{\rho g}+\frac{u^2+w^2}{2g}; \tag{2.8}$$

u and w are the velocity components, p is the pressure, ρ is the density, $h(s,t)$ denotes the flow depth, and p_h is the constant pressure at the free surface.

Let us assume shallow flow such that

$$\frac{\partial w}{\partial s}\simeq 0, \quad \frac{1}{g}\frac{\partial w}{\partial t}\simeq 0, \quad |w|\ll|u|;$$

we obtain from (2.2)

$$u(s,n,t)=\frac{u_0(s,t)}{1-\kappa n}, \tag{2.9}$$

from (2.1), (2.6) and (2.9)

$$w(s,n,t)=\left\{\frac{\ln(1-\kappa n)}{(1-\kappa n)\kappa}\right\}\frac{\partial u_0}{\partial s}-\frac{1}{\kappa^2}\frac{d\kappa}{ds}\left\{\frac{\ln(1-\kappa n)}{1-\kappa n}+\frac{\kappa n}{(1-\kappa n)^2}\right\}u_0, \tag{2.10}$$

and (2.4), (2.7), (2.8) and (2.9) yield

$$\frac{p(s,n,t)-p_h}{\rho g}=(h-n)\cos\theta+\frac{u_0^2}{2g}\left\{\frac{1}{(1-\kappa h)^2}-\frac{1}{(1-\kappa n)^2}\right\}. \tag{2.11}$$

Equations (2.9) and (2.10) define the influence of bed curvature on the velocity components, and (2.11) the pressure head due to both hydrostatic and curvature effects. Here bed velocity $u_0(s,t)$ and flow depth $h(s,t)$ are given by

$$\frac{1}{g}\frac{\partial u_0}{\partial t}+\frac{\partial E}{\partial s}=0, \quad (1-\kappa h)\frac{\partial h}{\partial t}+\frac{\partial q}{\partial s}=0, \tag{2.12), (2.13}$$

where the energy head E and flow per unit width q are

$$E(s,t) = \zeta + h\cos\theta + \frac{p_h}{\rho g} + \frac{u_0^2}{2g}(1-\kappa h)^{-2}, \tag{2.14}$$

$$q(s,t) = \int_0^h u\,dn = -\frac{u_0}{\kappa}\ln(1-\kappa h). \tag{2.15}$$

This is the system of equations obtained by Dressler (1978) using asymptotic methods. Equation (2.12) is a more compact form of his equation (13.01), and follows immediately from (2.3). Equation (2.13) may be interpreted as mass conservation, since $(\partial q/\partial s)\,ds$ is the net outflow rate and $(1-\kappa h)\,ds\,\partial h/\partial t$ is the rate of increase of free surface storage per unit width of channel. In deriving (2.13), we integrate (2.1) over the flow depth

$$\begin{aligned} -(1-\kappa h)\,w(s,h,t) &= \int_0^{h(s,t)} \frac{\partial}{\partial s}u(s,n,t)\,dn \\ &= \frac{\partial}{\partial s}\int_0^h u\,dn - u(s,h,t)\frac{\partial h}{\partial s} \\ &= \frac{\partial q}{\partial s} - u(s,h,t)\frac{\partial h}{\partial s}, \end{aligned}$$

and then invoke boundary condition (2.5). A more detailed discussion of the derivation of this system of equations may be found in Sivakumaran (1981).

For steady flow we note that the kinematic boundary condition (2.5) expressed as

$$\left.\frac{w}{u}\right|_{n=h} = \frac{1}{1-\kappa h}\frac{dh}{ds},$$

implies

$$|dh| \ll |(1-\kappa h)\,ds| \tag{2.16}$$

under the shallow-flow assumption $|w| \ll |u|$. We note that (2.16) is more readily satisfied when $\kappa < 0$.

3. Steady flow over a spillway crest

We apply the shallow-flow equations with bed curvature to steady flow over a spillway crest. Equations (2.14) and (2.15) reduce to (setting $p_h = 0$)

$$E = \zeta + h\cos\theta + \frac{u_0^2}{2g}(1-\kappa h)^{-2} = \text{constant}, \tag{3.1}$$

$$q = -\frac{u_0}{\kappa}\ln(1-\kappa h) = \text{constant}, \tag{3.2}$$

so that eliminating u_0 gives the equation for the upper nappe (defined by h)

$$E = \zeta + h\cos\theta + \frac{q^2\kappa^2}{2g}\{(1-\kappa h)\ln(1-\kappa h)\}^{-2}; \tag{3.3}$$

in dimensionless form

$$\left\{\frac{E}{H_d} - \frac{\zeta}{H_d}\right\} = \left\{\frac{\cos\theta}{\kappa H_d}\right\}\chi + F\left\{\frac{\kappa H_d}{(1-\chi)\ln(1-\chi)}\right\}^2, \tag{3.4}$$

H/H_d	$\frac{x_n}{H_d} = 0{\cdot}2$	$\frac{x_n}{H_d} = 1{\cdot}8$
0·50	−0·320	−0·016
1·00	−0·745	−0·059
1·33	−1·029	−0·110

TABLE 1.

where H_d denotes a reference head ('design head') and

$$\chi \equiv \kappa h, \quad F \equiv \frac{q^2}{2gH_d^3}. \tag{3.5}$$

The dimensionless pressure head at the bed ($n = 0$) is

$$\frac{p_0}{\rho g H_d} = \left\{\frac{E}{H_d} - \frac{\zeta}{H_d}\right\} - F\left\{\frac{\kappa H_d}{\ln(1-\chi)}\right\}^2, \tag{3.6}$$

where p_0 denotes the pressure at the bed.

Chow (1959) has summarized model tests by the U.S. Army Engineers Waterways Experiment Station of so-called WES shapes for high overflow spillways. We consider the case of vertical upstream face without piers described in § 14.6 of Chow (1959).

The spillway crest is given non-dimensionally by

$$\frac{\zeta}{H_d} = -\frac{1}{2}\left\{\frac{x}{H_d}\right\}^{1{\cdot}85}, \tag{3.7}$$

and experimental co-ordinates of the upper nappe profile are given for dimensionless operating heads (excluding the velocity head) $H/H_d = 0{\cdot}50$, $1{\cdot}00$ and $1{\cdot}33$. We consider the nappe co-ordinate domain $0{\cdot}2 < x_n/H_d < 1{\cdot}8$, for which the ranges of χ are summarized in table 1. It is notable that $\chi < -0{\cdot}85$ near the crest for $H/H_d = 1{\cdot}33$, somewhat *outside* the tentative range of validity suggested by Dressler (1978) for experimental check of the equations.

Setting $E = H$, we calculated the values of the parameter F (related to the Froude number) in (3.4) to fit the experimental upper nappe profiles at the nine tabular points $x_n/H_d = 0{\cdot}2(0{\cdot}2)1{\cdot}8$. The pointwise deviation of F from its average value is not more than 4%, as shown in figure 2. The inferred dimensionless flows per unit width ($F^{\frac{1}{2}}$) for operating heads $H/H_d = 0{\cdot}50$, $1{\cdot}00$ and $1{\cdot}33$ are $0{\cdot}163$, $0{\cdot}512$ and $0{\cdot}815$; weirs of simpler shapes are often used for flow measurements (see for example Ackers *et al.* 1978).† Further, a logarithmic plot of averaged $F^{\frac{1}{2}}$ against operating head H/H_d shown in figure 3 yields the formula

$$\frac{q}{(2g)^{\frac{1}{2}} H_d^{\frac{3}{2}}} = 0{\cdot}511\left\{\frac{H}{H_d}\right\}^{1{\cdot}647} \tag{3.8}$$

† Equation (3.4) defines the relation between $(E/H_d, F, \chi)$. To test this relation experimentally one must at least know either $(E/H_d, \chi)$ or (F, χ). For instance, given the energy (E/H_d) and the spillway and nappe profiles (χ for different x), equation (3.4) defines F uniquely; energy loss due to the build up of a turbulent boundary layer as we go down from the crest accounts for any slight error trend in estimating F (cf. figure 2). However, given either the energy or the flow (q), using (3.8) and (3.4) one can solve numerically for the unknown nappe.

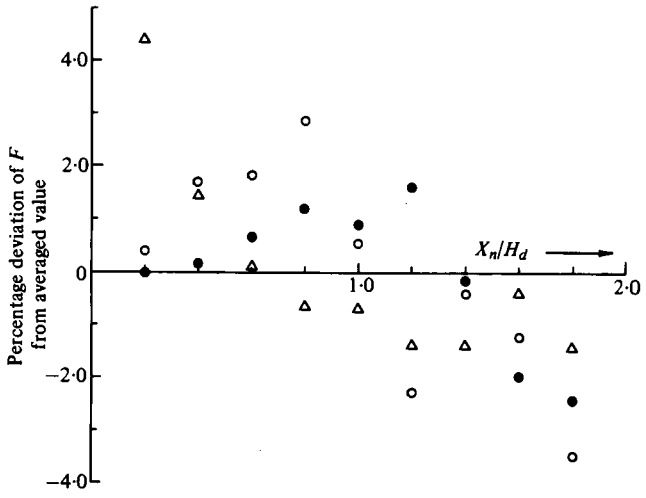

FIGURE 2. Point-wise percentage deviation of F: ○, $H/H_d = 0{\cdot}50$, $F_{av} = 0{\cdot}0266$; ●, $H/H_d = 1{\cdot}00$, $F_{av} = 0{\cdot}2622$; △, $H/H_d = 1{\cdot}33$, $F_{av} = 0{\cdot}6647$.

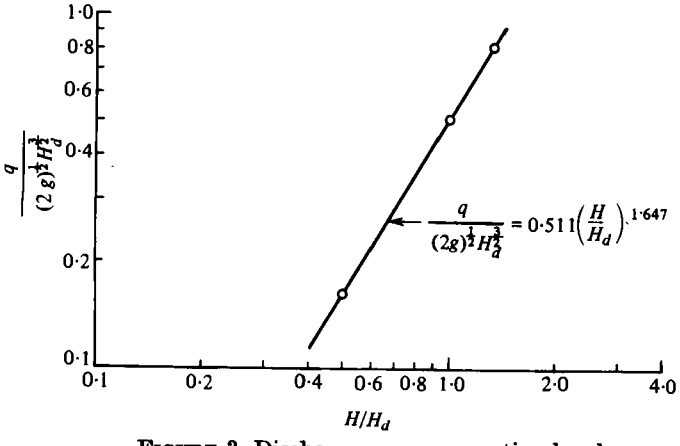

FIGURE 3. Discharge versus operating head.

or

$$\frac{q}{(2g)^{\frac{1}{2}}H^{\frac{3}{2}}} = 0{\cdot}511\left\{\frac{H}{H_d}\right\}^{0{\cdot}147}. \tag{3.8'}$$

Introducing a local Froude number as defined by Dressler (1978), *viz.*

$$\mathscr{F} \equiv \frac{u_0^2}{gh\cos\theta}, \tag{3.9}$$

with $E = H$ equation (3.1) reads

$$H = \zeta + \left\{1 + \frac{\mathscr{F}}{2(1-\chi)^2}\right\} h\cos\theta,$$

whence

$$\mathscr{F} = 2(1-\chi)^2\left\{\left(\frac{H}{H_d} - \frac{\zeta}{H_d}\right)\frac{\kappa H_d}{\chi}\sec\theta - 1\right\}. \tag{3.10}$$

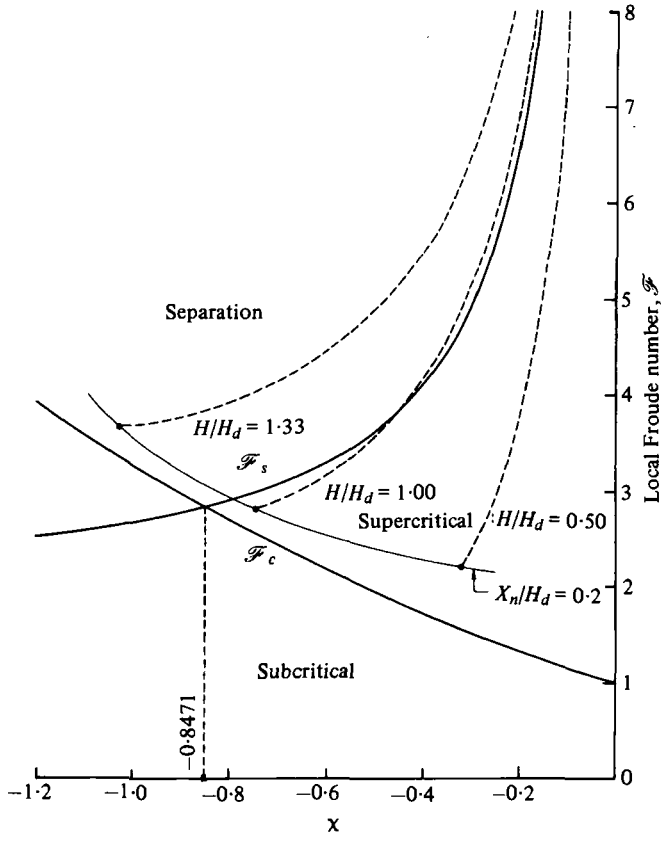

FIGURE 4. Curves for flow separation and critical flow. Subcritical: $\mathscr{F} < \mathscr{F}_c = -(1-\chi)^3 \ln (1-\chi)/\chi[1+\ln(1-\chi)]$. Separation: $\mathscr{F} \geqslant \mathscr{F}_s = -2(1-\chi)^2/\chi(2-\chi)$.

The local Froude number as a function of χ (shown in figure 4) corresponds to supercritical flow with or without separation.

Using the averaged values of F found from the upper nappe profiles, we computed theoretical pressure profiles from (3.6) for $H/H_d = 0{\cdot}50$, $1{\cdot}00$ and $1{\cdot}33$, to compare with the experimental profiles in the range $0 < x/H_d < 1{\cdot}2$ reproduced in Chow (1959), figures 14–13: see figures 5(*a*, *b*). These experimental pressure profiles at the bed are affected by separation at larger heads and build up of local turbulence, particularly behind curvature discontinuities that should be avoided (Rouse & Reid 1935) but are clearly indicated in Chow's figure. Slight modification of the results to allow for the influence of the neglected approach velocity head might be expected. We also fitted the experimental pressure profiles shown in Chow (1959) as best we could to (3.6), to obtain new parameter values $F^{*\frac{1}{2}} = 0{\cdot}160$, $0{\cdot}507$ and $0{\cdot}797$ for the respective dimensionless operating heads $H/H_d = 0{\cdot}50$, $1{\cdot}00$ and $1{\cdot}33$: we obtained

$$\frac{q}{(2g)^{\frac{1}{2}} H_d^{\frac{3}{2}}} = 0{\cdot}502 \left\{\frac{H}{H_d}\right\}^{1{\cdot}65} \tag{3.8''}$$

Further encouraging comparison with experiment is reported in a paper now in preparation.

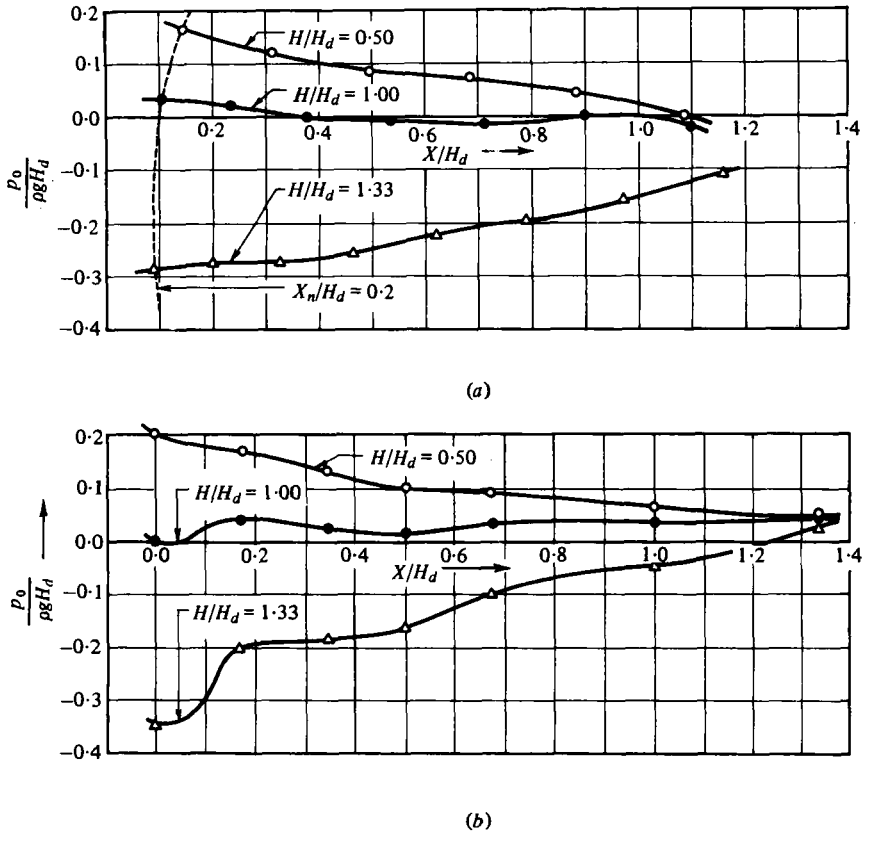

FIGURE 5. Pressure profiles along the spillway crest: (*a*) theoretical, and (*b*) experimental.

4. Steady flow over a spillway toe

Assuming negligible potential energy, various authors have given analytic solutions for steady ideal flow over a spillway toe. Douma (1954) and Balloffet (1961) used a 'free-vortex' approximation, and Henderson & Tierney (1963) used a hodograph transformation to study irrotational flow for large curvature. A detailed discussion of their assumptions may be found in Henderson (1966) and also in Dobson (1967), who computed solutions by finite difference methods.

The irrotational nature of the shallow flow equations implicit in (2.9) leads to an identical solution if the potential energy is neglected. It follows from the Bernoulli equation (cf. (2.8) or (3.1)) that the particle speed at the free surface is constant (u_1, say); hence from (3.2) and (2.11) we have the dimensionless curvature

$$a^{-1} \equiv \kappa h_1 = \Omega \ln \Omega^{-1}, \tag{4.1}$$

and the pressure coefficient

$$C_p \equiv \frac{p_0}{\frac{1}{2}\rho u_1^2} = 1 - \Omega^2, \tag{4.2}$$

where $\Omega = 1 - \kappa h_2$, p_0 is the bed pressure at the point of symmetry, and h_1, h_2 are the initial and central depths respectively (cf. figure 6). This solution is identical with

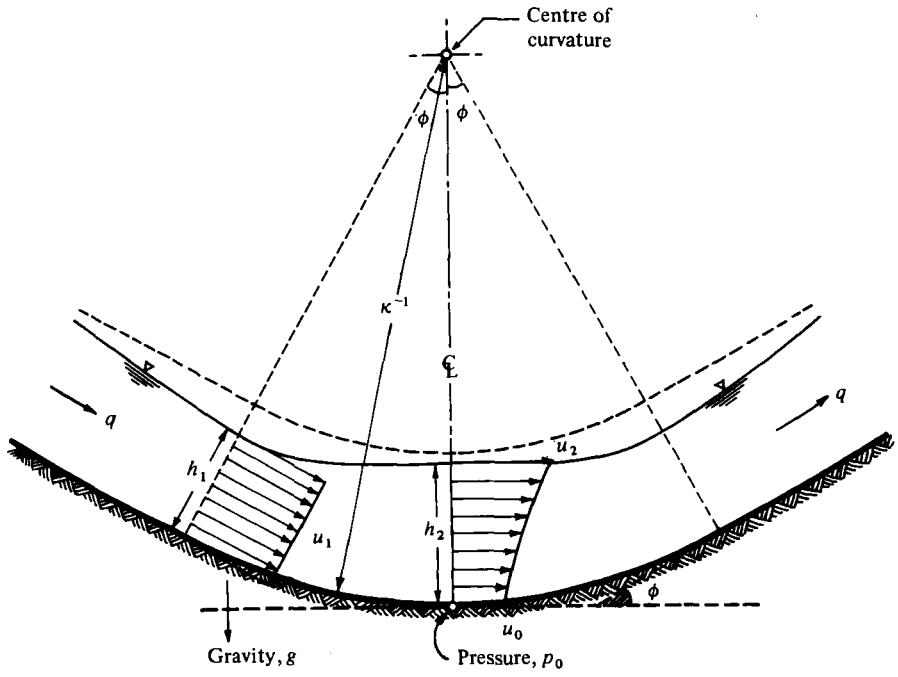

FIGURE 6. Flow at a spillway toe.

that of 'free-vortex' theory and is valid when $\kappa h_1 \lesssim \frac{1}{6}$ or $\kappa h_2 \lesssim 0{\cdot}185$ according to Henderson & Tierney (1963).

Of course the shallow-flow equations also readily permit a solution including the potential energy. In the symmetric case shown in figure 6 for example, it follows from (3.1) and (3.2) that

$$\frac{1}{(\Omega \ln \Omega)^2} = \alpha\Omega + \beta, \tag{4.3}$$

where $\alpha \equiv 2a^3 F_1^{-1}$, $\beta \equiv a^2 - 2a^2(a-1)\,F_1^{-1}\cos\phi$, $a \equiv (\kappa h_1)^{-1}$ as before, and $F_1 \equiv u_1^2/(gh_1)$.

The bed pressure at the point of symmetry (p_0) now consists of a hydrostatic component

$$p_s = \rho g h_2$$

and a centrifugal component

$$p_c = \tfrac{1}{2}\rho u_0^2\{(1-\kappa h_2)^{-2} - 1\};$$

or correspondingly

$$C_s \equiv \frac{p_s}{\frac{1}{2}\rho u_1^2} = \frac{2a}{F_1}(1-\Omega) \tag{4.4}$$

$$C_c \equiv \frac{p_c}{\frac{1}{2}\rho u_1^2} = (1-\Omega^2)\,(a\Omega \ln \Omega)^{-2}. \tag{4.5}$$

When the potential energy is neglected ($F_1 \to \infty$) the hydrostatic part vanishes, so that $C_p = C_c$. The root $e^{-1} \leqslant \hat{\Omega} < 1$ of (4.3) that corresponds to the low potential energy limit (infinite Froude number) described above is shown in figure 7. Corresponding centrifugal pressure profiles for various Froude numbers are shown in figure 8, and

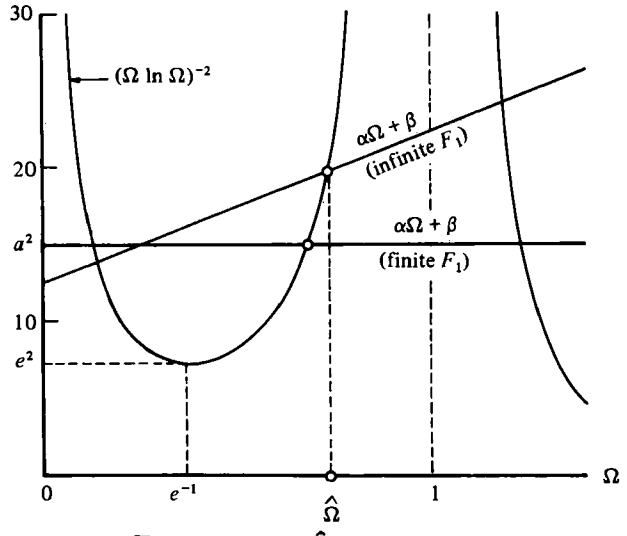

FIGURE 7. Root $\hat{\Omega}$ of equation (4.3).

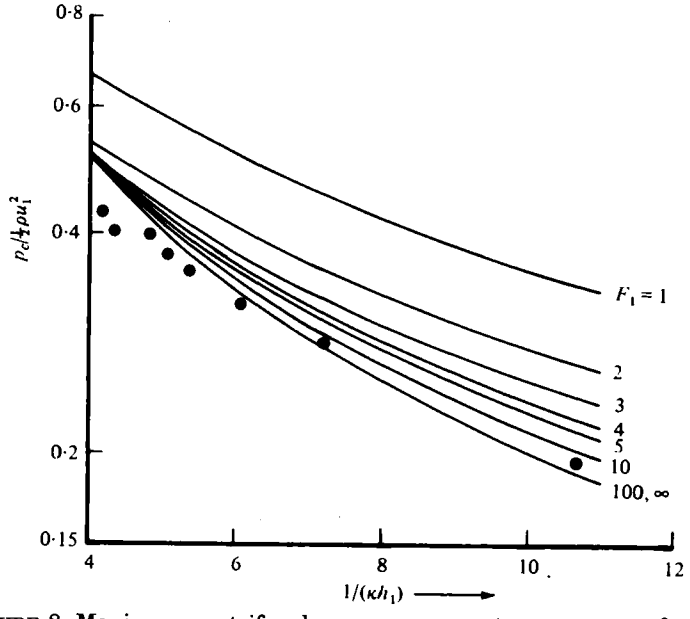

FIGURE 8. Maximum centrifugal pressure versus toe curvature, for $2\phi = 45°$. ●, experiment ($2\phi = 45°$), after Henderson & Tierney (1963).

we note that the bed pressure at the point of symmetry is increased when the potential energy is included. Thickening of the flow layer associated with increasing centrifugal pressure is illustrated in figure 9. We note that the solution validity is as before, and that we have continued to neglect surface disturbances that may occur at high Froude number.

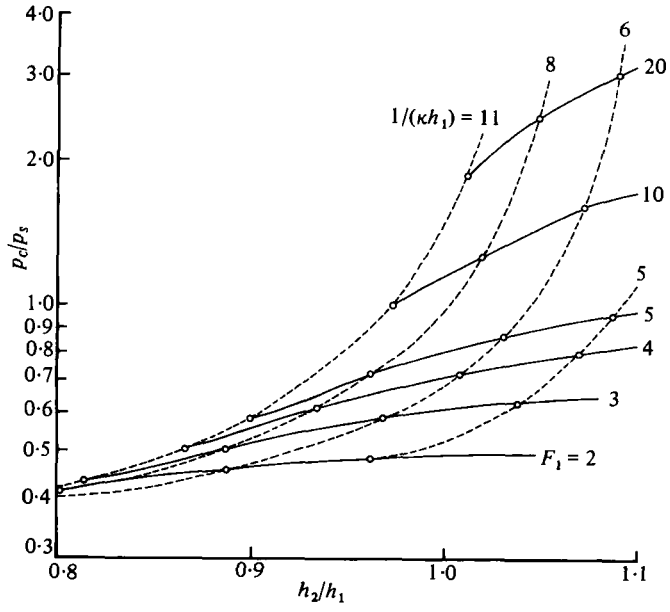

FIGURE 9. Flow layer thickening with increasing centrifugal pressure, for $2\phi = 45°$.

5. Conclusions

The derivation of recent shallow flow equations with bed curvature has been reviewed. It has been shown that these equations may be used to predict steady flow and pressure profiles over high overflow spillway crests or toes. Comparison with experiment for a tested spillway indicates that the equations are valid for quite large negative bed curvature (convex bottom), although limited to smaller positive bed curvature (concave bottom).

REFERENCES

ACKERS, P., WHITE, W. R., PERKINS, J. A. & HARRISON, A. J. M. 1978 *Weirs and Flumes for Flow Measurement.* Wiley.

BALLOFFET, A. 1961 Pressures on spillway flip buckets. *Proc. A.S.C.E.* **87** (HY5), 87–98.

CHOW, V. T. 1959 *Open Channel Hydraulics*, pp. 370–380. McGraw-Hill.

DOBSON, R. S. 1967 Some applications of a digital computer to hydraulic engineering problems. *Dept of Civil Engng, Stanford Univ. Tech. Rep.* no. 80, pp. 36–39.

DOUMA, J. H. 1954 Discussion on design of side walls in chutes and spillways. *Trans. A.S.C.E.* **119**, 364–368.

DRESSLER, R. F. 1978 New nonlinear shallow flow equations with curvature. *J. Hydraulic Res.* **16**, 205–220.

HENDERSON, F. M. 1966 *Open Channel Flow*, pp. 180–191. Macmillan.

HENDERSON, F. M. & TIERNEY, D. G. 1963 Flow at the toe of a spillway, II – The "solid toe" spillway. *La Houille Blanche* **1**, 42–50.

ROUSE, H. & REID, L. 1935 Model research on spillway crests, a study of pressure distribution and discharge as a function of crest design. *Civil Engng* **5**, 47.

SAINT-VENANT, B. de 1871 *C.R. Acad. Sci. Paris* **73**, 147–154, 237–240.

SIVAKUMARAN, N. S. 1981 Shallow flow over curved beds. D. Eng. thesis, Asian Institute of Technology, Bangkok, Thailand.